The Dynamic Behavior of Annexin V as a Function of Calcium Ion Binding: A Circular Dichroism, UV Absorption, and Steady-State and Time-Resolved Fluorescence Study

5 AUTHORS, INCLUDING:

Jana Sopkova-de Oliveira Santos
Université de Caen Normandie
128 PUBLICATIONS **1,618** CITATIONS

SEE PROFILE

Michel Vincent
Université Paris-Sud 11
97 PUBLICATIONS **1,911** CITATIONS

SEE PROFILE

Petr Pancoska
University of Pittsburgh
101 PUBLICATIONS **3,083** CITATIONS

SEE PROFILE

The Dynamic Behavior of Annexin V as a Function of Calcium Ion Binding: A Circular Dichroism, UV Absorption, and Steady-State and Time-Resolved Fluorescence Study

Jana Sopkova,[‡,§] Jacques Gallay,[*,‡] Michel Vincent,[‡] Petr Pancoska,[§] and Anita Lewit-Bentley[‡]

LURE, Centre Universitaire Paris-Sud, Bâtiment 209D, 91405 Orsay France, and Department of Chemical Physics, Charles University, Ke Karlovu 3, 12116 Prague, Czech Republic

ABSTRACT: The binding of calcium ions to annexin V in the absence of phospholipids has been studied by UV-difference spectroscopy, circular dichroism, and steady-state and time-resolved fluorescence. In the absence of calcium, the unique tryptophan 187, located in domain III of annexin V, is surrounded by a strongly hydrophobic environment, as indicated by its "blue" fluorescence emission maximum (325 nm). This corresponds well with the description of the structure determined by X-ray crystallography of several crystal forms. The Trp187 time-resolved fluorescence decay shows the existence of a fast (picosecond) excited-state reaction which can involve the formation of an H-bond between the indole NH group and the proximate ϵ-OH and/or α-carbonyl groups of Thr224. Titration with calcium tends to stabilize the overall structure, as shown by circular dichroism, while leading to large modifications of the local structure around Trp187 making it accessible to the solvent as shown by UV-difference spectra, circular dichroism spectra, and the displacement of its fluorescence emission maximum at saturating concentrations of calcium (350 nm). A rapid (picosecond) formation of an excited-state complex, probably involving one or a few water molecules of the solvation shell, is observed. These observations correlate well with the conformational change observed in crystal structures obtained in high calcium concentrations, involving the removal of Trp187 from the buried position to the surface of the molecule [Sopkova, J., Renouard, M., & Lewit-Bentley, A. (1993) *J. Mol. Biol. 234*, 816–825; Concha, N. O., Head, J. F., Kaetzel, M. A., Dedman, J. R., & Seaton, B. A. (1993) *Science 261*, 1321–1324]. In the solvent-exposed conformation, the indole ring becomes mobile in the subnanosecond and nanosecond time range. This conformational change and the increase in local flexibility can be important for the accommodation of the protein on the surface of phospholipid membranes.

Annexin V is a member of a class of homologous proteins that bind to membranes in a calcium-dependent manner [see Moss, S. E. (Ed.) (1992) for a recent review]. They are formed by a core 4- or 8-fold repeats of a highly conserved sequence of about 70 amino acids and a more variable N-terminal region, believed to confer different properties on the individual annexins. The calcium-binding properties and thus probably the phospholipid-binding properties are located in the core region.

The three-dimensional structure of human annexin V has been solved for four different crystal forms, obtained under different crystallization conditions: hexagonal (Huber *et al.*, 1990a), rhombohedral (Huber *et al.*, 1990b), monoclinic (Lewit-Bentley *et al.*, 1992), and triclinic (Sopkova *et al.*, 1993). The structures show that the sequence domains correspond to structural domains, with each consisting of five α-helices (A–E). The overall shape of the molecule is somewhat flat, with a concave surface with the N- and C-termini on one side and the calcium sites on the opposite, convex surface. The calcium ions were found in three sites in the rhombohedral form, in domains I, II and IV. In the monoclinic form, two calcium ions were found in domains I and IV, while the hexagonal form contained none. The calcium ions are bound to loops connecting helices A and B, with the extremely conserved sequence (L,M)-K-G-(L,A)-G-T and

(D,E) some 40 amino acids downstream. This calcium-binding configuration is different from the classical E–F hand-type (Kretsinger, 1987) but resembles that found in phospholipase A$_2$ (Dijkstra *et al.*, 1981). The three structures mentioned above resemble each other closely, with the main difference given by the relative position of domains I + IV and II + III in a hinge-bending-like motion.

The triclinic structure, solved recently (Sopkova *et al.*, 1993), binds one calcium ion in domain III and, with lower affinity, in domain I. The sequence of the major site in domain III is slightly different from the calcium-binding sequence defined above, *i.e.*, G-E-L-K-W-G. In annexin I, the W is replaced by K in this sequence, and its crystal structure shows one calcium ion bound there, in a configuration analogous to the calcium sites described in the earlier annexin V structures (Weng *et al.*, 1993). In human annexin V, this is the site of the unique tryptophan, whose side chain is buried in most crystal forms. In the triclinic crystal form, the formation of the calcium site in domain III is accompanied by a conformational change of this loop, thus bringing the tryptophan side chain onto the surface of the molecule (Sopkova *et al.*, 1993). In rat annexin V, whose sequence is identical to human annexin V in this region, an analogous observation was published recently (Concha *et al.*, 1993).

To understand the mechanism of this conformational change, a detailed spectroscopic study of the effect of calcium was performed, taking advantage of the presence of the single Trp[1] residue. Calcium binding was monitored by UV-

difference spectroscopy, circular dichroism, and steady-state fluorescence. In order to gain insight into the dynamics of the Trp187 microenvironment and the influence of calcium binding in terms of nanosecond or subnanosecond excited-state kinetics and rotational motions, time-resolved fluorescence decays were measured.

MATERIALS AND METHODS

Protein Preparation. Recombinant human annexin V was prepared as before (Maurer-Fogy *et al.*, 1988). In this procedure, all calcium is removed during the purification by EDTA and the protein is stored in the absence of calcium. The protein was incubated with an equimolar solution of dithiothreitol before use. For measurements of absorbance and circular dichroism, the protein solution contained 50 mM Tris-HCl buffer, pH 7.5 (buffer A). For all fluorescence measurements, the buffer was the same but with 0.15 M NaCl added (buffer B). The calcium solution used for the titrations was prepared by dissolving $CaCl_2$ in buffer A. All chemicals were of analytical grade purity, obtained from Merck, France.

Absorbance and Circular Dichroism (CD) Measurements. UV-difference absorption spectra were measured with a Specord M40 spectrophotometer (Carl Zeiss, Jena). The same amount of annexin V ($\sim$1 mg/mL) in 50 mM Tris-HCl, pH 7.45 (buffer A), was placed in the sample and reference beams. $CaCl_2$ was added to the sample and an equivalent volume of buffer A to the reference solution. Spectra were recorded in the 250–340-nm region, using quartz cuvettes with a 1-cm path length.

CD spectra were recorded with a dichrograph Mark V, Jobin Yvon (Longjumeau, France). The far-UV CD spectra were measured between 200 and 270 nm with a concentration of annexin V of 0.37 mg/mL, in a 0.1-cm optical path cuvette. The near-UV CD were measured between 250 and 310 nm with a protein concentration of 1.8 mg/mL, in a 1-cm optical path cuvette.

Temperature-Dependent Measurements. The temperature range used with the CD technique was 19–42 °C, controlled by a U10 thermostat (Medingen, Dresden) and monitored directly in the cuvette. Temperature-dependent CD spectra were recorded on samples with Ca-free annexin V at concentrations of 0.36 and 1.8 mg/mL for the amide and aromatic transition regions, respectively. Ca-saturated annexin V samples contained 0.23 and 1.69 mg/mL annexin V and 0.375 and 0.58 M $CaCl_2$ for measurements in the amide and aromatic transition regions, respectively.

Steady-State Fluorescence Spectroscopy. Tryptophan fluorescence emission spectra were recorded between 300 and 380 nm on a SLM 8000 spectrofluorometer (Urbana, IL) with an excitation wavelength of 295 nm (bandwith, 2 nm). Buffer blanks (buffer B) were always subtracted in the same experimental conditions. Rayleigh and Raman scattering were minimized by crossed Glan-Thompson polarizers. The protein concentration for all fluorescence measurements was $\sim$0.4 mg/mL in buffer B. The temperature of the sample was controlled with a water-circulating thermostat (Huber Ministat).

Data Analysis. Series of absorption, difference absorption, steady-state fluorescence, and circular dichroism spectra, as obtained in Ca-titration or temperature-dependent experiments, were analyzed by the principal component variant of

factor analysis, described in detail in Malinowski (1991). As the result of this treatment, spectra of each series are expressed as a linear combination of a few common orthogonal basic spectra. The coefficients in these linear combinations quantify the contributions of the respective basic spectra to any individual measured spectrum. By relating the coefficients to experimental variables (Ca concentration, temperature), the commonly used one-wavelength dependencies are replaced by the quantities depending on the correlated intensities in all measured wavelengths. The number of independent spectral components was determined using the indicator function (Malinowski, 1991) and provides information about the complexity of the molecular process underlying the observed spectral changes.

Time-Resolved Fluorescence Spectroscopy. For time-resolved measurements, the tryptophan residue was selectively excited by a pulsed excitation provided by the positron storage ring Super-ACO (anneau de collision d'Orsay) working in a two-bunch mode. The frequency of the excitation pulse was 8.33 MHz, and a typical value of 0.6 ns was monitored for the full width at half-maximum of the instrumental response. The excitation wavelength was selected at 295 nm (5-nm bandwidth) by a grating monochromator and vertically polarized through a Glan-Thompson prism. The decays of the parallel $I_{vv}(t)$ and perpendicular $I_{vh}(t)$ intensities were collected alternatively on the instrument setup, as previously described (Kuipers *et al.*, 1991), by the single-photon-counting method (Yguerabide, 1972; Wahl, 1975). The time resolution was 19 ps/channel in a 2K memory.

The temperature of the sample turret was controlled ($\pm$0.5 °C) by a water-circulating cryothermostat (Haake). Temperature measurements were performed in the sample cuvette with a digital thermometer (Omega) equipped with a thermistor probe (YSI). The temperature range studied was 5–35 °C.

The total fluorescence intensity decays $T(t)$ were reconstructed from the decays $I_{vv}(t)$ and $I_{vh}(t)$ as $T(t) = I_{vv}(t) + 2\beta_{corr}I_{vh}(t)$.

Analysis of the fluorescence intensity decay data as a sum of 150 exponentials was performed by the maximum entropy method (MEM) (Livesey *et al.*, 1986; Livesey & Brochon, 1987). The programs use the commercially available library of subroutines MEMSYS 5 (MEDC Ltd., U.K.). Optionally, MEMSYS 5 can handle a 150-dimensional vector, without any *a priori* assumption on the sign of each amplitude. It is worth emphasizing that all the analyses start from the first channel in which the fluorescence signal is above the noise level.

The fluorescence anisotropy decay parameters were calculated also by MEM. It was assumed that each type of excited state is responsible in the same way for each type of depolarization process and possesses the same fundamental anisotropy value A_0 (Vincent & Gallay, 1991). The $\alpha(\tau)$ profile was obtained from a first analysis of $T(t)$ by MEM and held constant in a subsequent and global analysis of $I_{vv}(t)$ and $I_{vh}(t)$ which provided the distribution $\beta(\theta)$ of correlation times; 100 rotational correlation time values, equally spaced in logarithmic scale, were used for the analysis of $\beta(\theta)$.

RESULTS

UV-Difference Absorption Spectra. The addition of Ca to annexin induces differences in the aromatic chromophore region (250–330 nm) with three negative maxima at 293, 285, and 275 nm. The increase in Ca concentration does not change in any observable extent either the positions of the
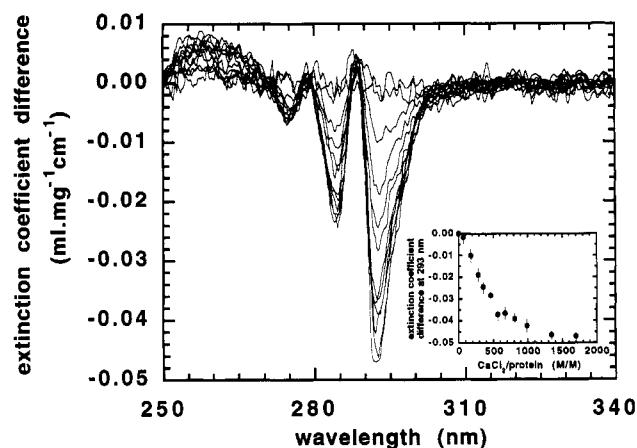

FIGURE 1: UV-difference absorption spectra of annexin V. Superposition of UV-difference absorption spectra of annexin V (1 mg/mL) as a function of calcium concentration (from 0 to 0.046 M). Inset: titration at 293 nm resulting from the difference spectra.

difference absorption peaks or their relative intensities. This is shown by the results of the principal component (PC) decomposition of the 11 difference absorption spectra, which gave only one significant component. The coefficients of this component reflect the Ca-dependent increase of the difference as shown in Figure 1. The plot of the dependence of the band magnitude at 293 nm on calcium addition is also shown in Figure 1 (inset).

Circular Dichroism in the UV Region. The overall band shape of the CD spectrum in the $n-\pi^*$ and $\pi-\pi^*$ transition region of the amide chromophores corresponds to the crystal structure of annexin V: it is typical of a protein with about 70% α-helical secondary structure. Upon the first addition of Ca (0.09 mM Ca into a 0.34 mg/mL (0.01 mM) solution of annexin V), we observe a minor increase of negative CD intensity at 221.5 nm (by *ca.* 5% of the original value) (Figure 2A). Upon further addition of Ca, the band shape of the amide UV CD spectrum remains highly conserved; there is no observable band shape change even in the difference CD spectra in this region.

The long-wavelength region of the Ca-free annexin V CD spectrum exhibits low-intensity bands of aromatic chromophores: a positive peak at 292 nm and negative ones at 286, 277, 268, and 262 nm. Contrary to the amide region, the Ca titration induces monotonic changes of CD band shape in this region (Figure 2B). By PC analysis, the series of 11 spectra in this region was found to be composed of two basic spectra, the second one being identical to the difference CD as calculated from the original CD curves (Figure 2C). The band shape of this difference basic spectrum describes the correlated intensity decrease of positive and negative maxima at 292 and 286 nm, respectively (at 58 mM Ca, it is down to 50% of the original intensities), accompanied by a small blue shift (1–2 nm; Figure 2B). No significant changes were observed for the Ca titration in the negative CD bands at 262, 268, and 277 nm. The plot of the dependence of the band magnitude at 292 nm on calcium addition is shown in Figure 2C (inset). The band at 292 nm corresponds to the tryptophanyl 0–0 ^1L_b band, and that at 286 nm is probably the tryptophanyl 0–1 ^1L_b band (Striekland, 1974).

Temperature-Dependent Spectra. In the amide transition region, an increase of the temperature from 18 to 42 °C induces a change of CD spectral intensity in both Ca-free and Ca-bound annexin V: a 5% and 8% relative decrease at 221.5 nm for Ca-bound and Ca-free samples, respectively. In the aromatic transition region, the trend of the variation (decrease
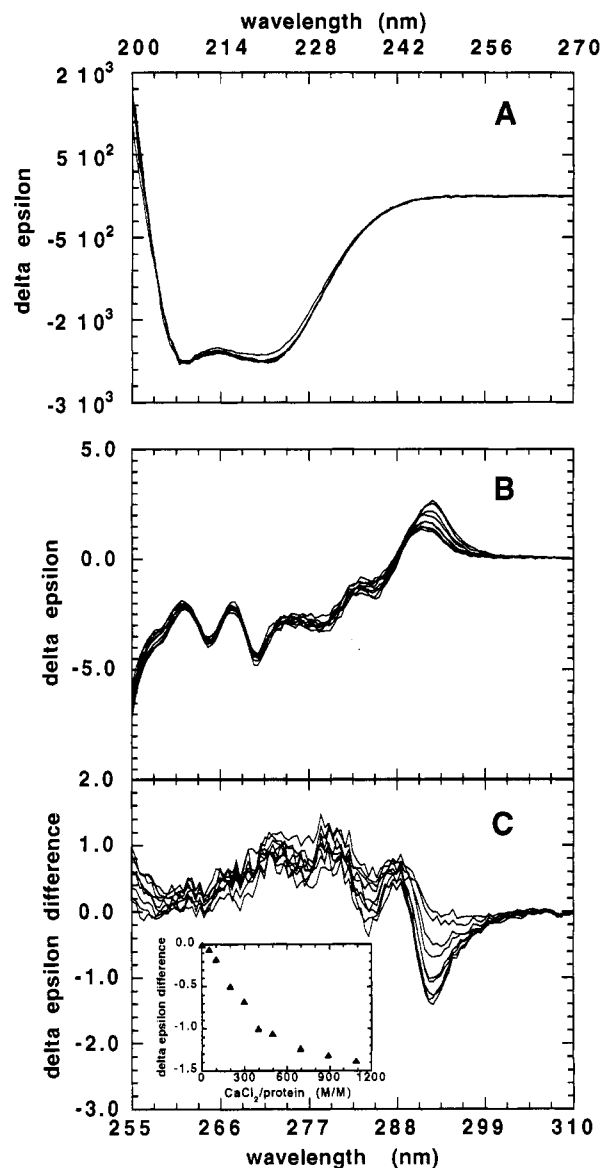

FIGURE 2: Circular dichroism of annexin V. (A) Far-UV CD spectra of the peptide groups of annexin V (0.37 mg/mL) as a function of calcium concentration (from 0 to 0.375 M). (B) Near-UV CD spectra of the aromatic residues of annexin V (1.8 mg/mL) as a function of calcium concentration (from 0 to 0.062 M). (C) Near-UV CD difference spectra as a function of calcium concentration. Inset: titration of the near-UV CD-difference spectra at 292 nm resulting from the difference spectra.

in intensity of all bands, most dominant at 292 nm) is exactly opposite. In the Ca-free sample, the intensity of the 292-nm band decreases only by 25% upon heating from 18 to 42 °C, while in the Ca-bound sample, this band looses 40% of its intensity under the same conditions.

For steady-state fluorescence spectra of Ca-free annexin, only a decrease of relative quantum yield upon heating was observed for the temperature range of 10–34 °C, with no observable shift of the fluorescence maxima. Moreover, no band shape modifications were discernible (after normalization, all fluorescence spectra were identical within experimental error).

Steady-State and Time-Resolved Fluorescence Measurements of Trp187 in Calcium-Free Annexin V. The steady-state fluorescence emission of Trp187 in annexin V is maximal at 325 nm (Figure 3), which characterizes an environment inaccessible to the bulk solvent, in agreement with previous results (Meers, 1990; Meers & Mealy, 1993). However, the
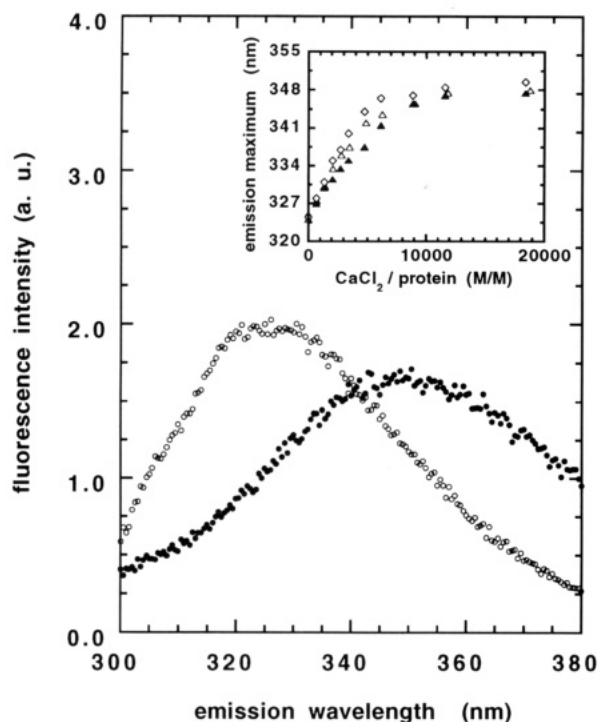
FIGURE 3: Fluorescence emission spectrum of Trp187 in annexin V: (O) calcium-free protein and (●) calcium-bound protein. Inset: variation of the fluorescence emission maximum as a function of the total calcium/protein mole ratio. Temperature: (△) 10 °C, (▲) 20 °C, and (◇) 30 °C. Excitation wavelength: 295 nm. Protein concentration: 0.4 mg/mL.
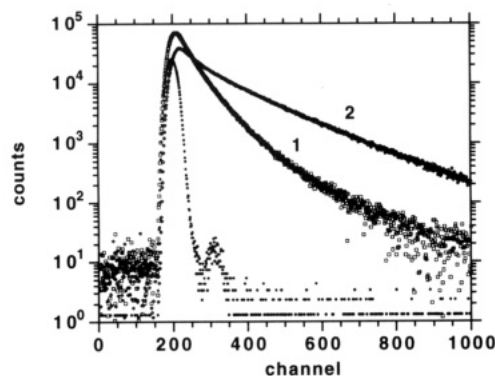

FIGURE 4: Fluorescence intensity decay of Trp187 in annexin V: curve 1, in the absence of calcium; curve 2, in the presence of calcium ions (200 mM). Excitation wavelength: 295 nm (bandwidth, 5 nm). Emission wavelength: 320 nm (bandwidth 10 nm) in the absence of calcium and 350 nm (bandwidth, 10 nm) in its presence. Temperature: 20 °C. Protein concentration: 0.4 mg/mL.

fluorescence decay monitored at 20 °C at the maximum of emission is not monoexponential and declines rapidly (Figure 4). This indicates that the environment is not inert and that quenching by close polar group(s) can occur in this hydrophobic pocket. Analysis of the data by MEM shows a heterogeneity of excited-state lifetimes (Figure 5). Three populations are present at 20 °C: one major component with a center of gravity of about 800 ps (70%) and two minor ones (center of gravity values 200–300 ps and 1.8 ns, respectively). Measurements at different emission wavelengths (Figure 5) show that a fourth long-lifetime component is distinguishable at long wavelengths, though its contribution is never higher than 2%. The center of gravity of each lifetime population remains at constant values, within the limit of experimental error, as a function of the emission wavelength, and their relative contributions are not changed significantly.
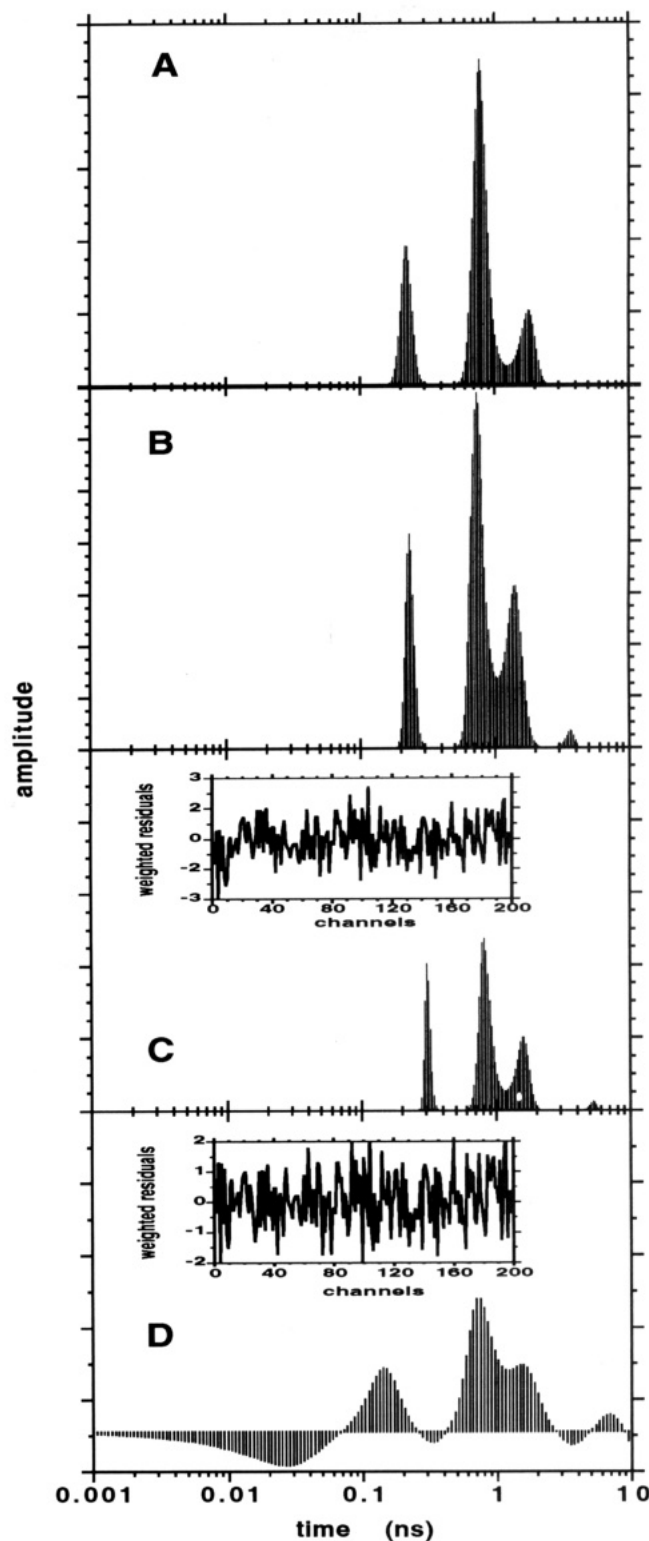

FIGURE 5: MEM-reconstituted excited-state lifetime distribution of Trp187 in annexin V in the absence of calcium as a function of the emission wavelength: (A) 320 nm, (B) 340 nm, (C) 365 nm (analysis using only positive preexponential terms), and (D) 365 nm (analysis without hypothesis on the sign of the preexponential terms). Insets: deviation function for each analysis. Excitation wavelength: 295 nm (bandwidth, 5 nm). Emission bandwidth: 10 nm. Temperature: 20 °C.

The fit of the data by the model using only positive preexponentials is quite satisfactory for all the measurements performed below 350 nm as emission wavelength, as estimated from the random pattern of the deviation function of the weighted residues for the whole time range of the measurement. However, in the red region of the fluorescence emission

spectrum (365 nm as emission wavelength), the fit of the data for the rising edge of the fluorescence curve is slightly improved by analysis with negative preexponentials (Figure 5), as shown by the pattern of the deviation function (Figure 5, insets). The major lifetime populations are less well resolved than in the first analysis: the longest lifetime appears only as a shoulder, and the shortest one is further displaced to shorter times. The poorer resolution is due to the broad time range used for the analysis (from 1 ps to 10 ns) in order to emphasize very short time constants.

At temperatures lower than 20 °C, this phenomenon is amplified (Figure 6). Analysis by MEM of the experimental data measured at an emission wavelength of 335 nm, to the red side of the maximum of emission, shows a poor fit of the data in the rising part of the experimental fluorescence decay (Figure 6A, insets) when using only positive preexponential terms. A significant improvement was observed when negative preexponential terms are included in the analysis (Figure 6B). The deviation function of the residuals becomes homogeneously distributed. The decay is described in this analysis by a broad excited-state lifetime distribution (center, 1.33 ns; maximum, 1.15 ns; half-width, 0.6 ns) and by a minor contribution (10%) of a shorter lifetime (0.26 ns). In the blue region of the emission spectrum, no negative preexponentials were detectable (not shown).

This phenomenon is progressively less and less detectable as a function of temperature (Figure 6). The major excited-state population remains with a center of around 1 ns. This value gradually decreases as a function of temperature.

Throughout the temperature range measured, the fluorescence anisotropy decay, measured in the short-wavelength region of the emission spectrum, does not show any fast motion of the Trp residue. Only one long rotational correlation time is needed to describe the decay (Figure 7). At 20 °C, the rotational correlation time value is 13 ns, corresponding to a monomer of 32 kDa with a 40% w/w hydration ratio as calculated from the Perrin–Einstein expression relating the rotational correlation time θ with the hydrodynamic volume V_h of the equivalent sphere and the viscosity/temperature factor: $\theta = V_h\eta/RT$ (Perrin, 1926). At 35 °C, a slight contribution of a 1.6-ns component is detected (data not shown). The initial anisotropy value is close to 0.2 as expected for Trp at a 295-nm excitation wavelength (Valeur & Weber, 1977). The indole ring, as well as the protein structure around it, is therefore essentially immobile on the nanosecond time scale in the calcium-free form of the protein. The plot of the rotational correlation time of the protein versus the viscosity/temperature is linear in the temperature range studied, but the ordinate at the origin is not zero as it should be for a rigid sphere (Figure 7, inset).

Steady-State and Time-Resolved Fluorescence Measurements of Trp187 in Calcium-Bound Annexin V. Specific perturbations of the Trp187 microenvironment by calcium ion binding are demonstrated by the steady-state fluorescence emission spectrum of the Trp residue (Figure 3). A progressive red shift of the fluorescence emission maximum is observed upon calcium binding which saturates at 350 nm (Figure 3, inset), in agreement with recent studies (Meers & Mealy, 1993).

The time-resolved fluorescence decay is also strongly modified as compared to that of the unliganded protein (Figure 4). Analysis of the decay by MEM shows a significant change in the excited-state lifetime distribution, mainly characterized by the appearance of a long lifetime (4 ns) (Figure 8). Such a change in the excited-state lifetime distribution coupled
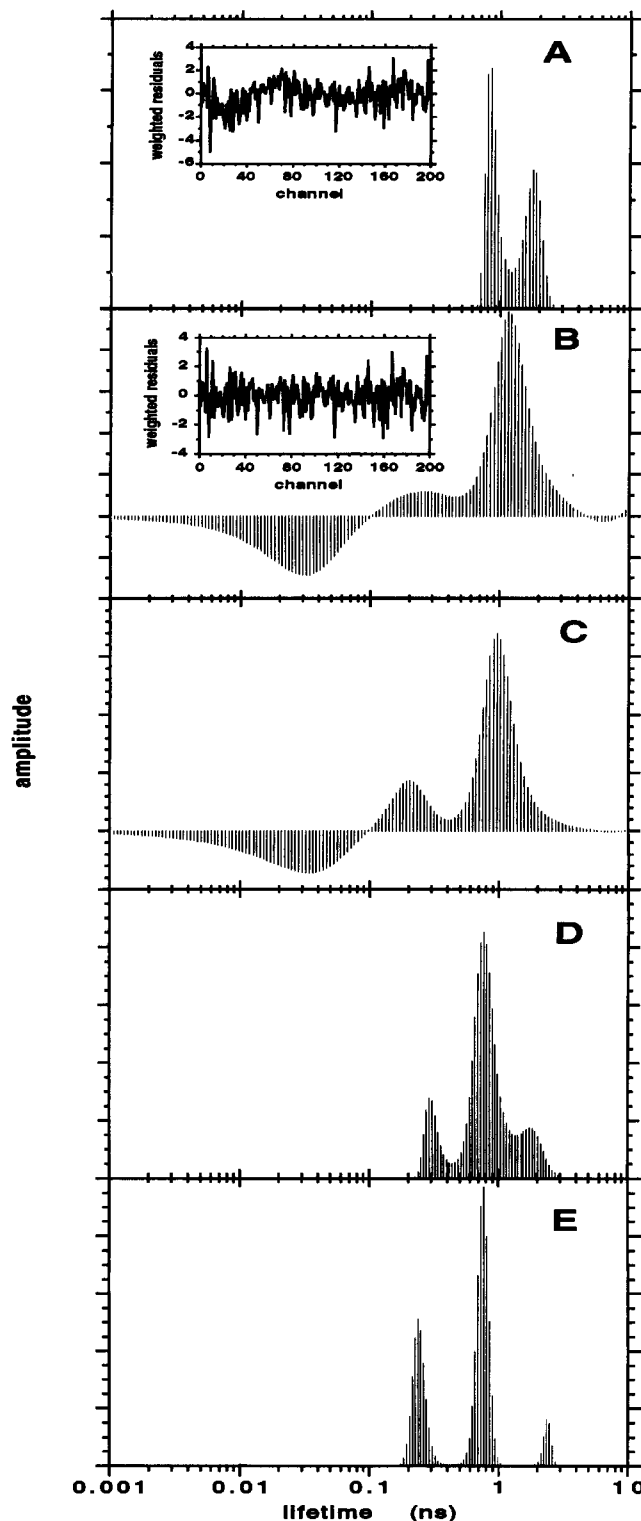

FIGURE 6: MEM-reconstituted excited-state lifetime distribution of Trp187 in annexin V in the absence of calcium at a 335-nm emission wavelength as a function of temperature: (A) temperature, 5 °C, analysis using only positive preexponential terms; (B) temperature, 5 °C, analysis without hypothesis on the sign of the preexponential terms; (C) temperature, 15 °C; (D) temperature, 20 °C; and (E) temperature, 35 °C. Excitation wavelength: 295 nm (bandwidth, 5 nm). Emission wavelength: 335 nm (bandwidth, 10 nm).

with a red shift of the fluorescence emission spectrum indicates a strong perturbation of the excited state by the polar solvent. The relative proportion of the long excited-state lifetime increases by a factor of 3.6 (from 0.18 to 0.65) as a function of the emission wavelength, at the expense of the shortest one (Figure 9A). Moreover, the fit to the experimental decay
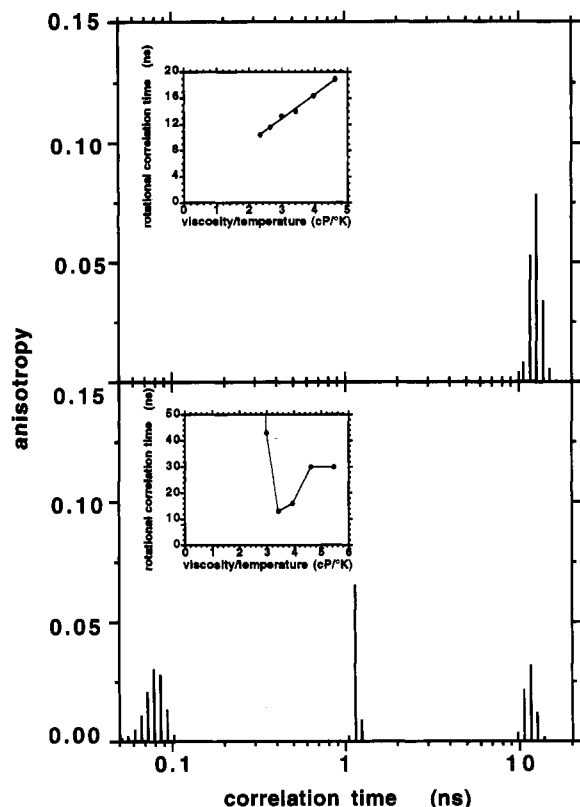
FIGURE 7: MEM-reconstituted correlation time distribution of Trp187 in annexin V: upper pannel, in the absence, and lower pannel, presence of calcium. Excitation wavelength: 295 nm (bandwidth 5 nm). Emission wavelength: 335 nm (bandwidth, 10 nm). Temperature: 20 °C. Insets: Perrin plot of the overall rotational correlation time of annexin V as a function of η/T.

curve at the red edge of the fluorescence emission spectrum is significantly improved at short times with negative preexponentials (Figure 9). This is shown both by the χ^2 values which decrease from 1.29 to 1.13 and the profile of the deviation function of the residuals (Figure 9B,C, insets). It is therefore likely that the indole moiety undergoes a stabilized excited state with water molecules.

In parallel with these important changes in the nature of the Trp187 microenvironment, a fast rotational motion of the indole ring (subnanosecond) as well as a slower local flexibility (nanosecond) is demonstrated by time-resolved fluorescence anisotropy decay measurements (Figure 7). The wobble angle of the fast subnanosecond rotation of the indole ring, calculated according to Kinosita et al. (1977), displays a value of 35°. The nanosecond rotational correlation times are extremely sensitive to temperature (variation from 4.6 ns at 5 °C to 1.2 ns at 35 °C). However, the overall rotational correlation time of the protein does not vary in a linear way as a function of the η/T factor.

DISCUSSION

Overall Protein Conformation. The overall conformation of the protein in solution is relatively stable as a function of temperature, both in the Ca-free and Ca-saturated forms. The secondary structure composition as seen by the practically invariant band shape and intensity of the CD spectra does not change more than 5–10% upon Ca binding. The minor "second-order" spectral changes observed after Ca is added could be attributed by their character and small intensity to the tertiary structure changes reported in the crystal structure data as changes in the relative positions of the I + IV and II
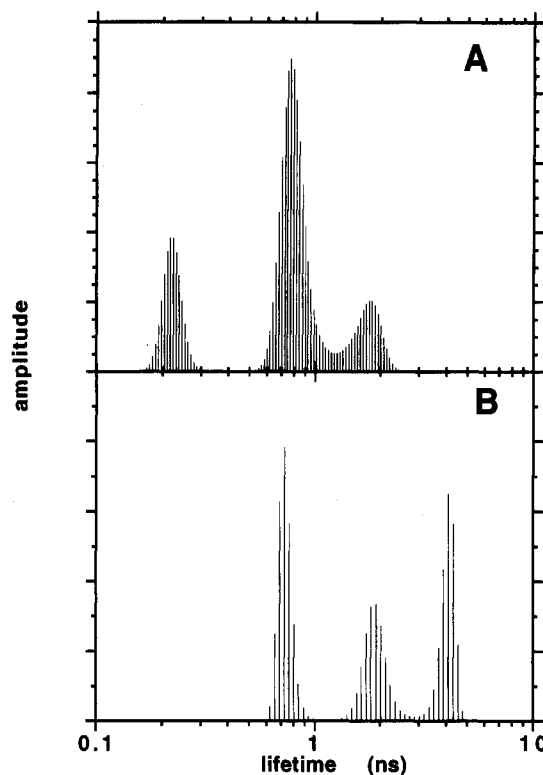

FIGURE 8: MEM-reconstituted excited-state lifetime distribution of Trp187 in annexin V: (A) in the absence of calcium and (B) in the presence of calcium at the respective maximum emission wavelength (325 and 350 nm).

+ III domains (Huber et al., 1990b), as well as within the domains. Such a movement can alter the segment–segment interactions (through distance and orientation change) and thus alter the rotational strength both in the amide and aromatic transition regions.

We suppose that this type of conformational change is also responsible for small correlated intensity differences in all aromatic bands with changes observed in the amide region for Ca-free annexin upon heating. The dominant contribution to the rotational strength of aromatic side chains is considered to be the dipole–dipole coupling of transition dipoles for neighboring aromatic groups. In contrast to some other proteins, the CD bands of aromatic groups in annexin V are well developed in the CD spectrum, which can be interpreted in terms of restricted mobility of these chains through hydrophobic interactions with the regular secondary structure domains of the protein. The extent of domain bending as seen in the crystals (Huber et al., 1990b; Lewit-Bentley et al., 1992) changes the distance and orientational parameters of the aromatic ring family only slightly and uniformly. Even the highest temperature (42 °C) applied in our study induces spectral changes consistent with this type of conformational change on the supersecondary structure level. The fact that the observed changes in the series of curves for different temperatures are of a simple "two-state" character (we can describe them entirely in terms of a linear combination of only two independent components) also favors the image of relative movement of rigid structural domains of the protein upon heating—a process not complicated by other conformational changes leading to an altered secondary structure.

Ca binding causes a similar change of the overall protein conformation, as monitored in the amide transition region by an intensity change induced by the first addition of Ca ions and then persisting. (It is worth noting here that our
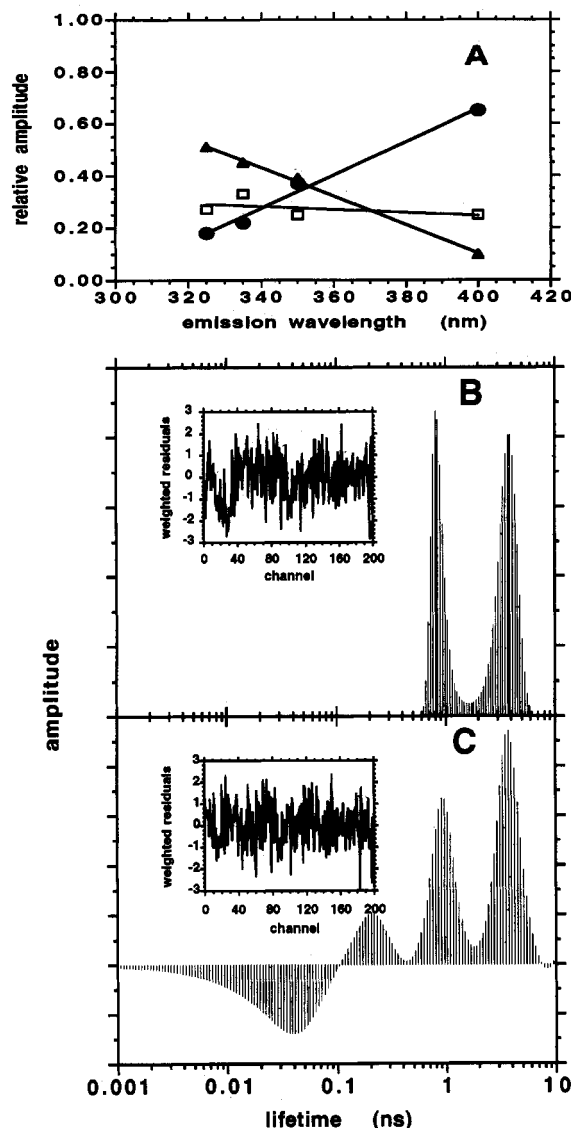
FIGURE 9: (A) Variation of the relative proportions of the excited-state lifetime populations as a function of fluorescence emission wavelength for the calcium–bound form of the protein: long lifetime (●), intermediate lifetime (□), and short lifetime (▲). (B) and (C) MEM-reconstituted excited-state lifetime distribution of Trp187 in annexin V in the presence of calcium at 400-nm emission wavelength: (B) analysis using only positive preexponential terms and (C) without hypothesis on their sign. Insets: deviation function for each analysis. Temperature: 20 °C.

experiments are performed in a large excess of Ca, so that most probably the other possible Ca-binding sites would also be occupied.) In the aromatic transition region, the monotonic intensity decrease which is exclusive for the two bands assigned to Trp reflects the more pronounced conformational change of this residue upon Ca binding. The two possible orientations of the polypeptide chain in the corresponding Ca-binding site with the buried and exposed Trp187 residues as found in the crystal structures (Sopkova *et al.*, 1993; Concha *et al.*, 1993) match perfectly the observed spectral changes in CD, absorption difference, and steady-state fluorescence spectra.

Temperature-dependent spectroscopic measurements of Ca-saturated annexin confirm the above picture. The most relevant result in this respect is the observation of opposite trends in the temperature-dependent CD spectral changes in the amide and aromatic regions for Ca-free and Ca-saturated samples. Ca binding apparently increases the overall stability of the protein tertiary structure as is seen from a relatively

smaller response of its amide CD spectrum to the increased temperature when compared to the Ca-free molecule. On the other hand, the relative extent of aromatic CD band variation is smaller for the Ca-free annexin than for the Ca-saturated protein upon heating. This probably reflects the immobilization of the aromatic residues in the protein interior in the Ca-free sample, as discussed above, and the more variable conformation of Trp187 after its unfolding by calcium binding, which correspondingly alters the aromatic region more for the heated Ca-saturated sample.

Local Dynamics of the Calcium-Free Form of the Protein. The steady-state and time-resolved fluorescence parameters reported here show that the local structure around the Trp187 residue in the calcium-free annexin V is hydrophobic and rigid on the nanosecond and subnanosecond time scales. These conclusions are in good agreement with the spectroscopic data discussed above and the crystallographic data. In the crystal structures prepared in low calcium concentration, hexagonal, rhombohedral (Huber *et al.*, 1990b), and monoclinic (Lewit-Bentley *et al.*, 1992), the loop connecting helices A and B of domain III is turned toward the interior of the molecule and the Trp187 side chain contained in this loop is buried within a hydrophobic pocket in the interior of domain III (Figure 10A). It is important to note here that the rhombohedral crystal form described by Huber *et al.* (1990b) was prepared in low calcium concentration and the crystal then soaked in high calcium concentration to saturate calcium sites accessible within the crystal lattice.

Despite the location of Trp187 within the interior of the protein, the time-resolved fluorescence intensity decays demonstrate the existence of several excited-state populations, indicating the existence of nonradiative exchange of energy with proximate polar groups. When no polar groups are present in the close proximity of the indole ring in a protein, like in the case of RNAse T1 (Heinemann & Saenger, 1982), the decay of Trp is a single exponential with a lifetime of 3.9 ns (Longworth, 1968; James *et al.*, 1985; Chen *et al.*, 1987). A detailed inspection of the neighborhood of the Trp187 side chain in the low-calcium crystal forms reveals a very small number of polar groups present within this pocket (Figure 10A): only the ε-OH and α-carbonyl groups of Thr224 are in close proximity to the indole ring and, in particular, to the indole ring nitrogen. The distances between the OH group of Thr224 and the indole ring nitrogen of Trp187 are 2.8 Å in the hexagonal and rhombohedral forms (Huber *et al.*, 1992) and 3.3 Å in the monoclinic form (Lewit-Bentley *et al.*, 1992), appropriate for the formation of hydrogen bonds in the ground state, providing deactivation channels in the excited state.

Moreover, below 20 °C, an extremely fast (picosecond) excited-state buildup takes place. This is shown by the detection at emission wavelengths longer than the maximum of emission, of a picosecond time constant associated with a negative preexponential. This reflects a rapid relaxation process occurring within the protein molecule, affecting the lifetime and energy level of the indole excited state. Simulated data curves have shown that recovery of such short time constants associated with negative preexponentials is possible with our instrument and MEM analysis (Vincent and Gallay, unpublished results).

The exact physical nature of this rapidly forming excited state is still a matter of debate. As the two extreme possibilities, it can involve either a nonspecific reorientation of polar groups around the excited chromophore (Ware *et al.*, 1971; DeToma *et al.*, 1976; DeToma, 1983) or a formation of a more specific excited-state complex ("exciplex") with a polar group of a
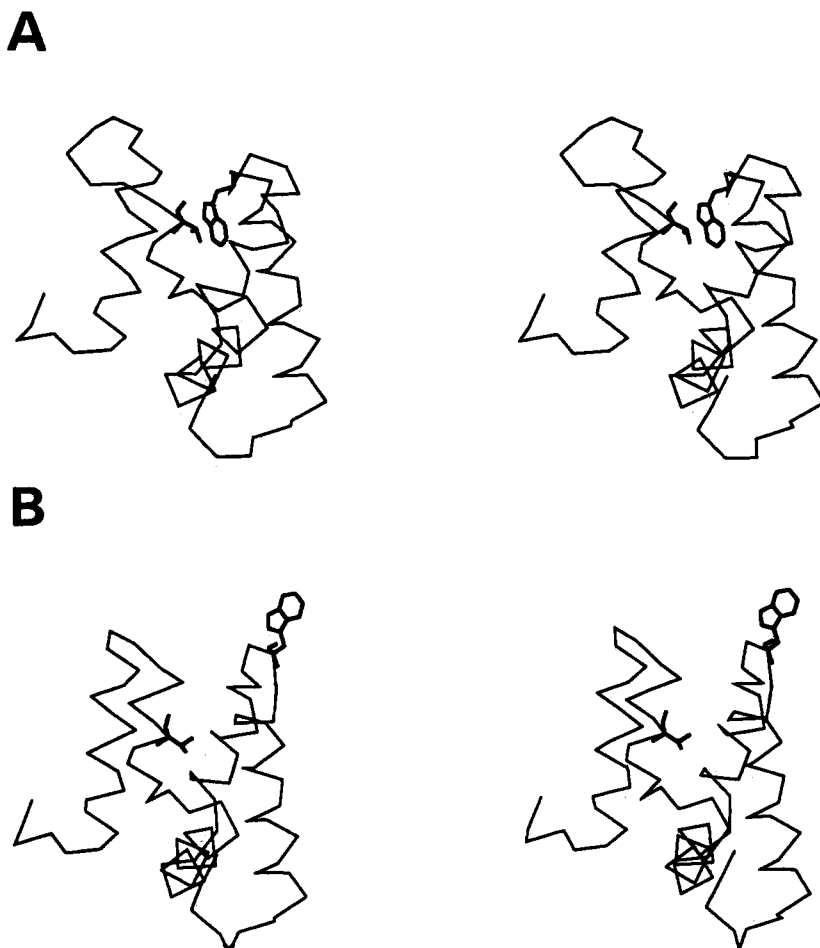
A

B

FIGURE 10: Stereo diagram Cα tracing of domain III in annexin V: (A) in the absence of calcium, with the Trp187 side chain buried, and (B) in the presence of high calcium concentration, with the Trp187 side chain exposed. The Trp187 and Thr224 side chains are superimposed.

molecule in close proximity (Ware, 1983). Both mechanisms are described by similar fluorescence kinetics, for the relaxed or complexed excited-state, respectively. In the simplest case of two states (Grinvald & Steinberg, 1974), it is characterized by a biexponential decay in the blue region of the fluorescence emission spectrum and by a difference of exponentials in the long-emission wavelength region. If a unique excited-state complex is formed, a single fast rate constant should be measured, whereas if interactions with several groups occur, a distribution of rates can be obtained.

In the specific case of Trp residue, the existence of an excited-state reaction and/or formation of a complex (exciplex) between indole or indole derivatives and polar groups of solvent molecules has long been suggested by steady-state fluorescence emission studies and was proposed as a plausible explanation for the large Stokes shift of the fluorescence emission spectra as a function of the solvent polarity (van Durren, 1961; Walker et al., 1966, 1967; Hopkins & Lumry, 1972; Hershberger & Lumry, 1976; Lumry, 1978; Hershberger et al., 1981). Time-resolved fluorescence measurements have provided kinetic arguments supporting this hypothesis (De Lauder & Wahl, 1971; Meech et al., 1982, 1983; Gudgin-Templeton & Ware, 1984). More recently, the existence of negative preexponential terms in the fluorescence decay of Trp in polar solvents including deuterated water (Willis et al., 1991), glycerol, and ethanol (Vekshin et al., 1992) has been demonstrated to occur at long fluorescence emission wavelengths (≥380 nm). Interestingly, the fluorescence decay of NATA in glycerol and ethanol at long emission wavelengths displayed such negative preexponential terms (Vekshin et al., 1992). To our

knowledge, the present results obtained on annexin V constitute the first reported example of an excited-state reaction occurring in a protein in a picosecond time range. The mechanism of the buildup process can involve excited-state proton transfer which is an important mechanism in the Trp photophysics (Demchenko, 1986), especially in the case of quenching by proton donors (Yu et al., 1992).

Coming back to annexin V, upon absorption of one photon by the indole ring, the H-bonds mentioned above can be transiently destabilized and rapidly reformed in the subnanosecond time scale. The preservation of the respective orientations of both groups, due to the rigidity of the local structure within the hydrophobic pocket, as shown by fluorescence anisotropy decay, can explain the relatively fast rate of the reaction. At higher temperatures, the excited-state lifetime distribution becomes different: three excited-state lifetime populations can be separated, indicating more structural heterogeneity around the Trp187 residue. The major component is the same as at lower temperature, but the excited-state buildup is no longer detectable. This suggests that it becomes too fast to be detected.

Effect of Calcium Binding on the Time-Resolved Fluorescence of Trp187. The excited-state properties of Trp187 are considerably modified in the calcium-bound form of the protein as well. The observation of a fast (picosecond) excited-state buildup, detectable at the red edge of the fluorescence emission spectrum (400 nm), reveals again the existence of a fast excited-state relaxation as in the calcium-free form of the protein. Although these fast excited-state reactions have never been clearly demonstrated by pulsed fluorescence in

pure water for Trp and NATA (Rayner & Szabo, 1978; Szabo & Rayner, 1980; Chang et al., 1983; Petrich et al., 1983; Willis et al., 1991; Vekshin et al., 1992), they have been recently observed in reverse micelles constituted of water and surfactant in organic solvents (Vincent, Vekshin, and Gallay, in preparation). This suggests that in the hydration shell of proteins, the mobility of water is reduced substantially to slow down the excited-state reaction with the indole ring, which thus can become experimentally detectable.

When crystals are prepared in high calcium concentrations, the loop connecting helices A and B of domain III becomes a calcium-binding loop situated on the surface of the molecule, with a conformation very close to the calcium-binding loops in the other annexin domains. The exposure of the loop on the molecular surface brings about the total exposure of the Trp187 side chain (Figure 10B) (Sopkova et al., 1993; Concha et al., 1993). The crystal packing shows that the indole does indeed make a large number of stabilizing contacts and hydrogen bonds with neighboring well-ordered water molecules (Sopkova et al., 1993).

In its exposed conformation, the Trp187 side chain exhibits a high mobility as shown by fluorescence anisotropy decay measurements. Fast subnanosecond and slower nanosecond motions are taking place in the new structure. The fastest motion is likely due to an averaging of the indole ring rotations around $C\alpha$–$C\beta$ and $C\beta$–$C\gamma$ bonds, while the nanosecond rotation reflects probably a local flexibility of the peptide segment containing the Trp187 residue. These two rotations are more sensitive to the viscosity/temperature factor (η/T) than the rotational correlation time for a Brownian motion. This indicates that the local protein conformation is flexible. This flexibility can also explain the nonlinear variation of the overall rotational correlation time of the calcium-bound protein as a function of the viscosity/temperature factor which shows a convex curvature toward the η/T axis. According to Weber (1953), this can be present only if the correlation times themselves are not linear function of η/T. The anisotropy decay measurements provide also information about the global size and therefore the association state of the protein. The data suggest the existence of an autoassociation process. This phenomenon, already described (Ahn et al., 1988), was also recently detected in NMR and neutron small-angle-scattering experiments in the presence of calcium (Neumann et al., in preparation).

In conclusion, our data obtained in solution show that the conformational change in domain III of annexin V, as described by the correlation and consistency of spectroscopic data with structural information obtained by X-ray crystallography of different crystal forms, is induced by calcium. In the calcium-free protein, the indole ring is immobilized and buried within the interior of the protein. According to the crystallographic structure, the indole nitrogen makes a hydrogen bond with the OH group of the Thr224 side chain or with the α-carbonyl group of the same residue. Excitation of the indole ring by UV light absorption disturbs this H-bond, which can be rapidly reformed in the picosecond time domain. The addition of calcium increases the stability of the overall conformation of the annexin V molecule. At the same time, a local conformational change that causes the formation of a calcium site in domain III brings the tryptophan onto the surface of the protein. The indole ring becomes extremely mobile and is in contact with solvent molecules of the hydration shell with which it undergoes a picosecond excited-state reaction which can be either a hydrogen-bonding, involving the ring nitrogen, or solvent-relaxed excited state. These modifications of the local protein conformation and dynamics may be relevant for the accommodation of the protein molecule on the surface of phospholipid membranes and thus to its biological function.

REFERENCES

Ahn, N. G., Teller, D. C., Bienkowski, M. J., McMullen, B. A., Lipkin, E. W., & de Haën, C. (1988) *J. Biol. Chem. 263*, 18657–18663.

Brisson, A., Moser, G., & Huber, R. (1991) *J. Mol. Biol. 220*, 199–203.

Chang, M. C., Petrich, J. W., Mc Donald, D. B., & Fleming, G. R. (1983) *J. Am. Chem. Soc. 105*, 3819–3824.

Chen, L. X.-Q., Longworth, J. W., & Fleming, G. R. (1987) *Biophys. J. 51*, 865–873.

Concha, N. O., Head, J. F., Kaetzel, M. A., Dedman, J. R., & Seaton, B. A. (1993) *Science 261*, 1321–1324.

Creutz, C. E. (1992) *Science 258*, 924–931.

De Lauder, W. B., & Wahl, Ph. (1971) *Biochim. Biophys. Acta 24*, 3153.

Demchenko, A. (1986) in *Ultraviolet Spectroscopy of Proteins*, Springer-Verlag, Berlin, Heidelberg.

DeToma, R. P. (1983) in *Time-Resolved Spectroscopy in Biochemistry and Biology, NATO Advanced Science Institute Ser. A: Life Sciences* (Cundall, R. B., & Dale, R. E., Eds.) Vol. 69, pp 393–410, Plenum Press, New York and London.

DeToma, R. P., Easter, J. H., & Brand, L. (1976) *J. Am. Chem. Soc. 98*, 5001–5007.

Dijkstra, B. W., Kalk, K. H., Hol, W. G. J., & Drenth, J. (1981) *J. Mol. Biol. 147*, 97–123.

Donovan, J. W. (1973) *Methods Enzymol. 27*, 497–525.

Grinvald, A., & Steinberg, I. Z. (1974) *Biochemistry 13*, 5170–5178.

Gudgin-Templeton, E. F., & Ware, W. R. (1984) *J. Phys. Chem. 88*, 4626.

Heinemann, U., & Saenger, W. (1982) *Nature 299*, 27–31.

Hershberger, M. V., & Lumry, R. W. (1976) *Photochem. Photobiol. 23*, 391.

Hershberger, M. V., Lumry, R. W., & Verall, R. (1981) *Photochem. Photobiol. 33*, 609.

Hopkins, T. R., & Lumry, R. W. (1972) *Photochem. Photobiol. 15*, 555.

Huber, R., Römisch, J., & Paques, E. P. (1990a) *EMBO J. 9*, 3867–3874.

Huber, R., Schneider, M., Mayr, I., Römisch, J., & Paques, E. P. (1990b) *FEBS Lett. 275*, 15–21.

Huber, R., Berendes, R., Burger, A., Schneider, M., Karshikov, A., Luecke, H., Römisch, J., & Paques, E. (1992) *J. Mol. Biol. 223*, 683–704.

Ichiye, T., & Karplus, M. (1983) *Biochemistry 22*, 2884–2893.

James, D. R., Demmer, D. R., Steer, R. P., & Verall, D. E. (1985) *Biochemistry 24*, 5517–5526.

Kinosita, K., Jr., Kawato, S. & Ikegami, A. (1977) *Biophys. J. 20*, 289–305.

Kretsinger, R. H. (1987) *Cold Spring Harbor Symp. Quant. Biol. 52*, 499–510.

Kuipers, O. P., Vincent, M., Brochon, J. C., Verheij, H. M., de Haas, G. H., & Gallay, J. (1991) *Biochemistry 30*, 8771–8785.

Lewit-Bentley, A., Morera, S., Huber, R., & Bodo, R. (1992) *Eur. J. Biochem. 210*, 73–77.

Livesey, A. K., & Brochon, J. C. (1987) *Biophys. J. 52*, 693–706.

Livesey, A. K., Licinio, P., & Delaye, M. (1986) *J. Chem. Phys. 84*, 5102–5107.

Longworth, J. W. (1968) *Photochem. Photobiol. 7*, 587–596.

Lumry, R. (1978) *Photochem. Photobiol. 27*, 819–840.

Malinowski, E. R. (1991) in *Factor Analysis in Chemistry*, 2nd ed., p 109, John Willey & Sons, New York.

Maurer-Fogy, I., Reutelingsperger, C. P. M., Peiters, J., Bodo, G., Stratowa, C., & Hauptman, R. (1988) *Eur. J. Biochem. 174*, 585–592.

McMahon, L. P., Colucci, W. J., McLaughlin, M. L., & Barkley, M. D. (1992) *J. Am. Chem. Soc. 114*, 8442–8448.

Meech, S. R., Phillips, D., & Lee, A. G. (1982) *Chem. Phys. Lett. 92*, 523–527.

Meech, S. R., Phillips, D., & Lee, A. G. (1983) *Chem. Phys. 80*, 317–328.

Meers, P. (1990) *Biochemistry 29*, 3325–3330.

Meers, P., & Mealy, T. (1993) *Biochemistry 32*, 5411–5418.

Moss, S. E. (Ed.) (1992) in *The Annexins*, Portland Press Ltd., London.

Perrin, F. (1926) *J. de Physique 7*, 390–401.

Petrich, J. W., Chang, M. C., McDonald, D. B., & Fleming, G. R. (1983) *J. Am. Chem. Soc. 105*, 3824–3832.

Rayner, D. M., & Szabo, A. G. (1978) *Can. J. Chem. 56*, 743.

Schlaepfer, D. D., Mehlman, T., Burgess, W. H., & Haigler, H. T. (1987) *Proc. Natl. Acad. Sci. U.S.A. 84*, 6078–6082.

Sopkova, J., Renouard, M., & Lewit-Bentley, A. (1993) *J. Mol. Biol. 234*, 816–825.

Striekland, E. H. (1974) *Crit. Rev. Biochem. Mol. Biol. 2*, 113.

Szabo, A. G., & Rayner, D. M. (1980) *J. Am. Chem. Soc. 102*, 554–563.

Valeur, B., & Weber, G. (1977) *Photochem. Photobiol. 25*, 441–444.

Van Durren, B. L. (1961) *J. Org. Chem. 26*, 2954–2960.

Vekshin, N., Vincent, M., & Gallay, J. (1992) *Chem. Phys. Lett. 199*, 459–464.

Vincent, M., & Gallay, J. (1991) *Eur. Biophys. J. 20*, 183–191.

Wahl, Ph. (1975) in *New Techniques in Biophysics and Cell Biology* (Pain, M., & Smith, B., Eds.) Vol. 2, pp 233–285, John Wiley and Sons Inc., London.

Walker, M. S., Bednar, T. W., & Lumry, R. J. (1966) *J. Chem. Phys. 45*, 3455.

Walker, M. S., Bednar, T. W., & Lumry, R. J. (1967) *J. Chem. Phys. 47*, 1020.

Ware, W. R. (1983) in *Time-Resolved Spectroscopy in Biochemistry and Biology, NATO Advanced Science Institute Ser. A: Life Sciences*, (Cundall, R. B., & Dale, R. E., Eds.) Vol. 69, pp 341–361, Plenum Press, New York and London.

Ware, W. R., Lee, S. K., Brant, G. J., & Chow, P. P. (1971) *J. Chem. Phys. 54*, 4729.

Weber, G. (1953) *Adv. Protein Chem. 8*, 415–459.

Weng, X., Luecke, H., Song, I. S., Kang, D. S., Kim, S.-H., & Huber, R. (1993) *Protein Sci. 2*, 448–458.

Willis, K. J., Szabo, A. G., & Kracjarski, D. T. (1991) *Chem. Phys. Lett. 182*, 614–616.

Yguerabide, J. (1972) *Methods Enzymol. 26*, 498–578.

Yu, H.-T., Colucci, W. J., McLaughlin, M. L., & Barkley, M. D. (1992) *J. Am. Chem. Soc. 114*, 8448–8454.